Two-photon Light Trigger Sirna Transfection of Cancer Cells Using Non-Toxic Porous Silicon Nanoparticles

Arnaud Chaix, Eduardo Cueto-Diaz, Sofia Dominguez-Gil, Chantelle Spiteri, Laure Lichon, Marie Maynadier, Xavier Dumail, Dina Aggad, Anthony Delalande, Aurélie Bessière, et al.

Two-photon light trigger siRNA transfection of cancer cells using non-toxic porous silicon nanoparticles

Arnaud Chaix, [a§] *Eduardo Cueto-Diaz,* [a§] *Sofia Dominguez-Gil,* [a§] *Chantelle Spiteri,* [b] *Laure Lichon*[d], *Marie Maynadier,* [c] *Xavier Dumail,* [a] *Dina Aggad,* [d] *Anthony Delalande,* [e] *Aurélie Bessière,* [a] *Chantal Pichon,* [e] *Ciro Chiappini,* [b] *Michael J. Sailor,* [f] *Nadir Bettache,* [d] *Magali Gary-Bobo,* [d] *Jean-Olivier Durand,* [a] *Christophe Nguyen,**[d] *Frédérique Cunin**[a]

A. Chaix, E. Cueto-Diaz, S. Dominguez-Gil, A. Bessière, J.O. Durand, F. Cunin

ICGM, Univ. Montpellier, CNRS, ENSCM, Montpellier 34293, France

E-mail: (frederique.cunin@enscm.fr)

C. Spiteri, C. Chiappini

Centre for Craniofacial and Regenerative Biology, King's College London, SE1 9RT, London, UK

London Centre for Nanotechnology, King's College London, WC2R 2LS, London, UK

M. Maynadier

NanoMedSyn Avenue Charles Flahault, 34093 Montpellier Cedex 05, France

L. Lichon, D. Aggad, N. Bettache, M. Gary-Bobo, C. Nguyen

IBMM, Univ. Montpellier, CNRS, ENSCM, 34093 Montpellier, France

E-mail: (christophe.nguyen@umontpellier.fr)

A. Delalande, C. Pichon

This article has been accepted for publication and undergone full peer review but has not been through the copyediting, typesetting, pagination and proofreading process, which may lead to differences between this version and the Version of Record. Please cite this article as doi: 10.1002/adhm.202301052.

1. ART ARNm, Inserm UMS55 and University of Orléans, F-45071, Orléans cedex 02, France

2. Institut Universitaire de France, 1 rue Descartes, F-75035 Paris, France

M. J. Sailor

University of California, San Diego, Department of Chemistry and Biochemistry, 9500 Gilman Drive, m/c 0358, La Jolla, CA 92093-0358, USA.

§ Contributed equally to this work

Keywords: ((3–7 keywords, not capitalized, plural, separated by commas, no full stop))

Gene delivery, two-photon excitation, porous silicon nanoparticle, siRNA transfection, non-viral vectors, photo-activable nanoparticles, photo-assisted therapy.

((Abstract text. Maximum length 200 words. Written in the present tense.))

The concept of using two-photon excitation in the NIR for the spatiotemporal control of biological processes holds great promises. However, its use for the delivery of nucleic acids has been very scarcely described and the reported procedures are not optimal as they often involve potentially toxic materials and irradiation conditions.

In this work, we prepare a simple system made of biocompatible porous silicon nanoparticles (pSiNP) for the safe siRNA photocontrolled delivery and gene silencing in cells upon two-photon excitation. PSiNP are linked to an azobenzene moiety, which possess a lysine group (pSiNP@ICPES-azo@Lys) to efficiently complex siRNA. Non-linear excitation of the two-photon absorber system (pSiNP) followed by intermolecular energy transfer (FRET) to trans azobenzene moiety, result in the photoisomerization of the azobenzene from trans to cis and in the destabilization of the azobenzene-siRNA complex, thus inducing the delivery of the cargo siRNA to the cytoplasm of cells. Efficient silencing in MCF-7 expressing stable firefly luciferase with siRNAluc against luciferase is observed. Furthermore, siRNA against inhibitory apoptotic protein (IAP) leads to over 70% of MCF-7 cancer cell death. The developed technique using two-photon light allows a unique high spatiotemporally controlled and safe siRNA delivery in cells in few seconds of irradiation.

1. Introduction

Gene therapy is a rapidly evolving therapeutic treatment consisting in the delivery of exogenous nucleic acid sequences designed specifically to target the diseased tissues. Gene delivery has been originally efficiently performed with viral systems. [1] However, they may exert immunologic and oncogenic adverse effects. Non-viral gene delivery systems, despite their current lower efficiency in terms of transfection, offer to overcome most of the shortcomings displayed by viral vectors, i.e. severe immune responses, low carrying capacity, small scale production, and high production cost. [2] In particular, inorganic nanoparticles and their intrinsic physical properties at the nanoscale are intensively being assessed. [3]

Porous silicon nanoparticles (pSiNP) are fully biodegradable, and nontoxic *in vivo*. [4] In addition pSiNP can be excited by near infrared (NIR) two-photon excitation (TPE) light [5] thus offering additional possibilities for light triggered treatment, based on tissue-penetrable NIR light response. Light triggered systems are indeed very potent to spatiotemporally control biological processes. [6] Pioneering work with cationic azobenzene-based systems was efficient in photocontrolling the transcription/translation of nucleic acids [7] through reversible isomerization of azobenzene upon UV-Vis irradiation; the systems were however not evaluated in cells. Few examples of cell transfection using light triggered nucleic acid delivery systems have been described and the field has been comprehensively reviewed. [8] The major works were reported so far with UV-Vis light, [9] and different mechanisms are used to photocontrol the delivery of nucleic acids including photocleavage of light-sensitive groups (such as ortho-nitrobenzyl), photochemical internalization, plasmonic-heated systems or isomerization of photoswitch molecules. However, poor tissue penetration and tissue damage with UV-Vis light represent a strong limitation for biological application. Recent works adapted these mechanisms to the NIR in order to overcome the limitations of UV-Vis light. Up-converting nanoparticles, which convert NIR light to UV-Vis light, are able to cleave nitrobenzyl groups. This feature led to the design of different systems for siRNA and photomorpholinos delivery. [10] Host-guest interactions between cyclodextrin and azobenzene covalently linked to siRNA have also been described using upconverting nanoparticles. [11] However, lanthanides-based nanoparticles could be toxic and not biodegradable, which could be a limitation for their use in biological media. [12] Plasmonic

systems have been described for NIR light-induced photothermal control of gene silencing with siRNA, [13] but gold nanoparticles are not biodegradable. Interestingly, TPE combines unique features with NIR excitation, high temporal and tri-dimensional (micron scale) spatial resolutions, thus a potent mean for the specific delivery of nucleic acids. However very few examples of TPE-induced nucleic acid delivery have been described. The direct two-photon cleavage of 4,5-dimethoxy-2-nitrobenzyl group [9j, 14] has been reported twice for nucleic acid delivery systems, but since this group possesses a very low two-photon decaging cross-section, [15] very long times of irradiation (hour) were needed with the risk of causing damages to the cells. Finally, FRET was recently described with a two-photon-induced charge-variable conjugated polyelectrolyte brush, with high two-photon absorption cross-section, to a nitrobenzyl-based side chain for siRNA delivery in cancer cells upon TPE at 720 nm for one hour, however 720 nm is the beginning of the tissue transparency window, which is not optimal. [16]

Herein we describe an efficient, simple system made of non-toxic pSiNP, for the safe siRNA photocontrolled delivery and gene silencing in cells upon TPE. Azobenzene functionalized with lysine was grafted on pSiNP and the construction efficiently complexed siRNA through non-covalent interactions between lysine and siRNA. PSiNP could act as a two-photon transducer[5] to the azobenzene moiety, which has a limited two-photon absorption cross-section. [17] Delivery of siRNA in MCF-7 Luc breast cancer cells, and luciferase gene silencing was triggered in cells by the photo-isomerization of the lysine-functionalized azobenzene groups upon TPE, with resonance energy transfer from pSiNP. In addition, pSiNP-mediated delivery of siRNA (IAP) to MCF-7 cells resulted in the cancer cells apoptosis, demonstrating the anticancer biological efficiency of the siRNA/pSiNP nanosystem under TPE. These results constitute the first example of high-efficiency siRNA transfection using TPE activated non-toxic porous Si nanoparticles.

2. Results and discussion

2.1. Preparation and characterization of the nanoformulations

Azobenzene functionalized with lysine was first prepared by coupling Boc-Lys(Boc)-OH amino-acid to 4,4'-diaminoazobenzene according to a procedure described in the experimental methods part and in ESI, (Figure S1, S2 and S3A). The obtained product azo@Lys(diBoc) was then reacted with isocyanatopropylethoxysilane (ICPES) [18] prior to be grafted to pSiNP by silanisation chemistry on the silicon hydroxide groups natively present at the surface of the pSiNP. Deprotection in a solution of TFA led to the final as-called pSiNP@ICPES-azo@Lys formulation (Figure 1. A and 1. B, ESI Figure S3). Two other formulations were prepared including bare pSiNP (pSiNP), and pSiNP grafted with azobenzene via ICPES linker [19] and without amino-acid (pSiNP@ICPES-azo) (Figure 1. B, ESI Figure S4). In addition, one extra formulation was synthesized where azobenzene spacer was replaced by benzidine spacer for control transfection experiments, as benzidine does not undergo trans-cis isomerization under light irradiation (Figure 1. B). In this case, the lysine amino-acid was first coupled to benzidine by coupling reaction between 4-4' diaminodiphenyl with Boc-Lys(Boc)-OH. The obtained new product, as called, benz@Lys(diBoc) was characterized by NMR spectroscopy and high-resolution mass spectroscopy (see experimental methods part and ESI Figure S5 and S6). Benz@Lys(diBoc) was then reacted with ICPES prior to be grafted to pSiNP by silanisation. Deprotection in a solution of TFA led to pSiNP@ICPES-benz@Lys formulation (Figure 1. B, ESI Figure S7 and S8). In this study, pSiNP were produced according to previously published procedure, by electrochemical etching of boron-doped crystalline silicon wafer followed by ultrasonic fracture.[5] pSiNP of 164 nm in size with a polydispersity of 0.18 and with average pore diameter of 19.5 nm were obtained. Because of the synthesis method (top down), pSiNP exhibit a fully open porosity, with large mesopores accessible to molecules and biomolecules infiltration. Characterizations by dynamic light scattering (DLS) and transmission electron microscopy (TEM) are described in the experimental methods and presented in Figure 1.C and 1.E respectively; nitrogen sorption analysis are presented in ESI, Figure S10. In addition, no significant cytotoxicity was observed neither for MCF-7 cells (Human breast adenocarcinoma) nor for HUVEC (endothelial) cells incubated during 72 h with increasing concentrations of pSiNP. Around 20% of cell death was observed for a concentration of 150 $\mu g.ml^{-1}$ for MCF-7 cells (Figure 1.D).

The nanoparticle formulations were characterized before and after grafting of the ICPES-modified moieties (i.e. ICPES-azo, ICPES-azo@Lys(diBoc) and ICPES-benz@Lys(diBoc)). Covalent grafting of the

ICPES-modified moieties was confirmed by diffuse reflectance infrared Fourier transform spectroscopy (DRIFTS) on the relevant formulations (ESI, Figure S12, S13 and S14). Zeta potential measurements also confirmed successful chemical functionalization of the nanoparticles, with an increase of the surface charge from -16.5 mV to +20.4 mV and to +43.1 mV for pSiNP, pSiNP@ICPES-azo@Lys, and pSiNP@ICPES-benz@Lys respectively, due to the presence of the ammonium groups of lysine amino-acid. Such positive surface charges are necessary for further complexation of siRNA on the nanoparticles. In contrast, pSiNP@ICPES-azo maintained a negative surface charge of -20.4 mV due to the hydroxide groups remaining at the pSiNP surface or forming during silanisation (ESI, Table S1). Dispersibility of the nanoparticles was observed for the four formulations (pSiNP, pSiNP@ICPES-azo, pSiNP@ICPES-azo@Lys and pSiNP@ICPES-benz@Lys) in biologically relevant conditions, at a concentration of 1 $mg.ml^{-1}$ in water (NaCl 1mM, pH 7.2), at room temperature. Furthermore, DLS indicated an increase in the hydrodynamic diameter of the nanoparticles after grafting of the ICPES-modified moieties from 164 nm to 295 nm, 255 nm and 293 nm, for pSiNP, pSiNP@ICPES-azo, pSiNP@ICPES-azo@Lys, and pSiNP@ICPES-benz@Lys respectively (ESI, Figure S11). Here, this increase in diameter of 131 nm for pSiNP@ICPES-azo is attributed to a slight aggregation of the nanoparticles. Less aggregation is observed for pSiNP@ICPES-azo@Lys which exhibit a highly positive surface charge. In addition, pSiNP are not spherical shaped nanoparticles, their non-isotropy could explain some discards of the hydrodynamic diameter values when surface charges, thus interactions, are modified. Furthermore, the polydispersity indices of the nano-formulations are lower than 0.2, indicating that the colloidal dispersions are stable. Finally, the amount of grafted ICPES-azo, ICPES-azo@Lys and of ICPES-benz@Lys was determined spectrophotometrically after dissolution of the pSiNP@ICPES-azo, pSiNP@ICPES-azo@Lys, and pSiNP@ICPES-benz@Lys nanoparticles in basic medium (see experimental methods part and ESI, Table S2). A higher amount of ICPES-azo@Lys was grafted on pSiNP compared to ICPES-benz@Lys, which is consistent with the higher surface charge for the pSiNP@ICPES-azo@Lys formulation measured by Zeta potential.

The complexation of siRNA with the nanoparticle formulations was studied by agarose gel retardation assay for pSiNP@ICPES-azo@Lys and pSiNP@ICPES-benz@Lys, which exhibit a favourable positive surface charge for complexation with siRNA. For each compound, three weight ratios were tested,

namely 1/5, 1/25 and 1/50 (siRNA/pSiNP). Both formulations pSiNP@ICPES-azo@Lys and pSiNP@ICPES-benz@Lys, efficiently complexed siRNA at ratios 1/25 and 1/50, while no complexation was observed at ratio 1/5 (Figure 2. A, and 2. B). As the complexation is related to the number of positive charges (from the nanoparticles) versus negative charges (from siRNA), the absence of complexation at ratio 1/5 is attributed to an excess of siRNA regarding the quantity of pSiNP. Indeed, in wells 4 and 9 the luminescent bands corresponding to siRNA for the ratio 1/5 are observed. The absence of alteration in the migration of siRNA demonstrates that no complexation occurs with pSiNP at this ratio. In contrast, for ratios 1/25 or 1/50, the disappearance of siRNA band confirms the complexation of siRNA with pSiNP, that blocks the migration through the agarose gel. SiRNA is expected to be immobilized at both the internal and external surface of the pSiNP@ICPES-azo@Lys and pSiNP@ICPES-benz@Lys nanosystems, where the positive charges of the Lysine groups are.

2.2. Photocontrolled siRNA delivery upon TPE and transfection efficiency

The delivery of siRNA to cells, triggered by TPE, was investigated with luciferase-expressing MCF-7 breast cancer cells (MCF-7 Luc). siRNA sequence was chosen to specifically target the luciferase gene (siLuc 5'-AACGTACGCGGAATACTTCGA-3') expressed in the MCF-7 Luc cells. siRNA was mixed for 30 min at room temperature with pSiNP, pSiNP@ICPES-azo, pSiNP@ICPES-azo@Lys, and pSiNP@ICPES-benz@Lys at 1/25 weight ratio for which efficient complexation was observed. The siRNA-nanocomplexes were then incubated with MCF-7 Luc for 5 hours at 40 $\mu g.ml^{-1}$. Irradiation of the cells upon TPE was performed using a confocal microscope and a wavelength of 800 nm (1100 mW output at lens). Cells received 3 laser pulses of duration 1.57 s each. Expression of luciferase was recorded after two days. Negative control experiments indicated that irradiation itself did not affect the cells (Figure 2. C). In addition, bare pSiNP as well as functionalized pSiNP, namely pSiNP@ICPES-azo, pSiNP@ICPES-azo@Lys, and pSiNP@ICPES-benz@Lys did not affect the cells either, in the presence or not of irradiation, as luciferase expression was not observed to be significantly changed (Figure 2. C). The transfection efficiency of free siRNA and of the four nano-formulations mixed with siRNA in 1/25 weight ratio was then studied and the effect of TPE at 800 nm was recorded (Figure 2. D). Free siRNA

did not induce gene-silencing effect. In addition, neither pSiNP + siRNA nor pSiNP@ICPES-azo + siRNA induced inhibition of luciferase expression, as such negatively charged formulations did not complex and transport siRNA. In contrast, extinction of 38% of the luciferase expression was observed with pSiNP@ICPES-azo@Lys + siRNA, indicating efficient transfection of the cells upon TPE. In previous work, we have shown that pSiNP is able to absorb TPE light and transfer its energy to anchored absorbing molecules.[5] Here siRNA delivery is attributed to the photo-isomerization of the azobenzene groups upon TPE, after resonance energy transfer from pSiNP to the azobenzene. The resonance energy transfer mechanism was supported by the fluorescence quenching of pSiNP in the presence of azobenzene and by the obtained Stern-Volmer linear plot (ESI, Figure S15). In our system, pSiNP act as a two-photon antennae able to transfer the energy to the azobenzene moiety, which can undergo trans-cis isomerization. Additionally, a control experiment was performed with pSiNP@ICPES-benz@Lys + siRNA. Unlike azobenzene, benzidine does not undergo photo-isomerisation. Irradiation of pSiNP@ICPES-benz@Lys + siRNA with TPE did not reveal gene silencing effect, also demonstrating the role of azobenzene and its photo-isomerisation in the release mechanism of siRNA (Figure 2. D). Moreover, no production of reactive oxygen species (ROS) was observed, indicating that endosomal escape is not due to photochemical internalization (PCI) and thus confirming that trans-cis isomerization of azobenzene is essential. In the present study, the photo-controlled delivery of siRNA is based on the property of azobenzene possessing a cationic moiety to switch its affinity for nucleic acids, when undergoing a trans-cis isomerization. This is known since the work of D. Baigl. [7] With azobenzene possessing a cationic moiety, the trans conformation is compacted with nucleic acids, but the isomerization of azobenzene to the cis conformation unfolds nucleic acids, resulting in a weaker binding. In the present system, the release of siRNA is attributed to the photo-induced conformation change of azo@lys, which isomerizes in the cis configuration with a lower affinity for siRNA. [7] The endocytosis of the siRNA was confirmed by fluorescence confocal microscopy on MCF-7 human breast cancer cells stained with lysotracker (Figure 2. E (A)) and incubated with either free siRNA (160 nM) or siRNA complexed with pSiNP@ICPES-azo@Lys (ratio 1/25) for 24 hours. Green siRNA-ATTO was used in this experiment. Images presented in Figure 2.E indicate successful internalization of siRNA (Figure 2. E (B)), with a significant increase when complexed with pSiNP@ICPES-azo@Lys nanoparticles (Figure 2. E (C)). Finally, cell viability experiments in the presence or not of siRNA and of TPE irradiation

indicated no toxicity of the nano-formulations to the cells, making them very interesting non-viral gene vectors (ESI, Figure S16).

2.3. Photocontrolled anticancer biological efficiency

In order to further investigate the anticancer efficiency of the pSiNP@ICPES-azo@Lys-siRNA formulation, a siRNA directed against inhibitory apoptotic protein (IAP) was loaded into pSiNP@ICPES-azo@Lys nanovector. When available in cancer cell cytoplasm, siRNA (IAP) can block the mRNA coding for IAP and thus remove inhibition of apoptosis occurring in the cancer cells. In this experiment, pSiNP of 190 nm in size with average pore diameter of 13 nm, as-called pSiNPa, were prepared and chemically functionalized with ICPES-azo@Lys(diBoc) following the procedures previously presented and as described in the experimental methods. Prior to chemical functionalization and ligand deprotection, the absence of cytotoxicity for the pSiNPa used in the treatment conditions was confirmed. Figure 3A shows that increasing concentrations of pSiNPa incubated for 72 h with MCF-7 and HUVEC cells did not induce significant toxicity, with approximatively 20% of cellular death at the highest concentration of 150 $\mu g.ml^{-1}$. The pSiNPa and pSiNPa@ICPES-azo@Lys were characterized by transmission electron microscopy, nitrogen adsorption analysis, dynamic light scattering, Zeta potential measurements and FTIR spectroscopy (ESI, Figure S17-S20 and table S3). They featured comparable textural and surface chemical properties as pSiNP and pSiNP@ICPES-azo@Lys previously presented. The complexation of siRNA (IAP) with pSiNPa@ICPES-azo@Lys was then studied by agarose gel retardation assay for three siRNA/nanoparticle weight ratios (1/10, 1/25 and 1/50). Typically, a fixed concentration of siRNA (IAP) was incubated with increasing concentrations of pSiNPa@ICPES-azo@Lys and deposited on agarose gel. Efficient complexation of siRNA (IAP) was obtained at ratio 1/50 (Figure 3.B). This ratio was retained to evaluate the biological efficiency of the pSiNPa@ICPES-azo@Lys-siRNA(IAP) nanocomplex to kill cancer cells compared to free siRNA (IAP).

In this study, the nanocomplexes were incubated with MCF-7 for 5 hours at 40 $\mu g.ml^{-1}$ and irradiation of the cells upon TPE irradiation was performed at a wavelength of 800 nm (3 laser pulses of duration 1.57 s each). Cell viability was recorded after two days (Figure 3.C). Figure 3.C shows that laser

irradiation did not induce significant cell death neither in control cells nor in cells incubated with free siRNA (IAP). In addition, the pSiNPa@ICPES-azo@Lys-siRNA (IAP) complex was non-toxic to the cells in the absence of irradiation. A killing biological activity of about 20% was observed with free siRNA (IAP) incubated with the cells, but, as mentioned, no cell death due to siRNA(IAP) was observed in the absence of irradiation, when it was loaded in the nanoparticles, indicating that siRNA is not released and is maintained inactive in the nanoparticles. However, upon TPE excitation, 74% cell death was observed, highlighting the siRNA (IAP) release and apoptosis restoration by blocking mRNA (IAP). These results demonstrate siRNA controlled release and cancer cell killing using non-toxic photoactivable pSiNPa@ICPES-azo@Lys nanocomplexes with focused TPE light for the first time.

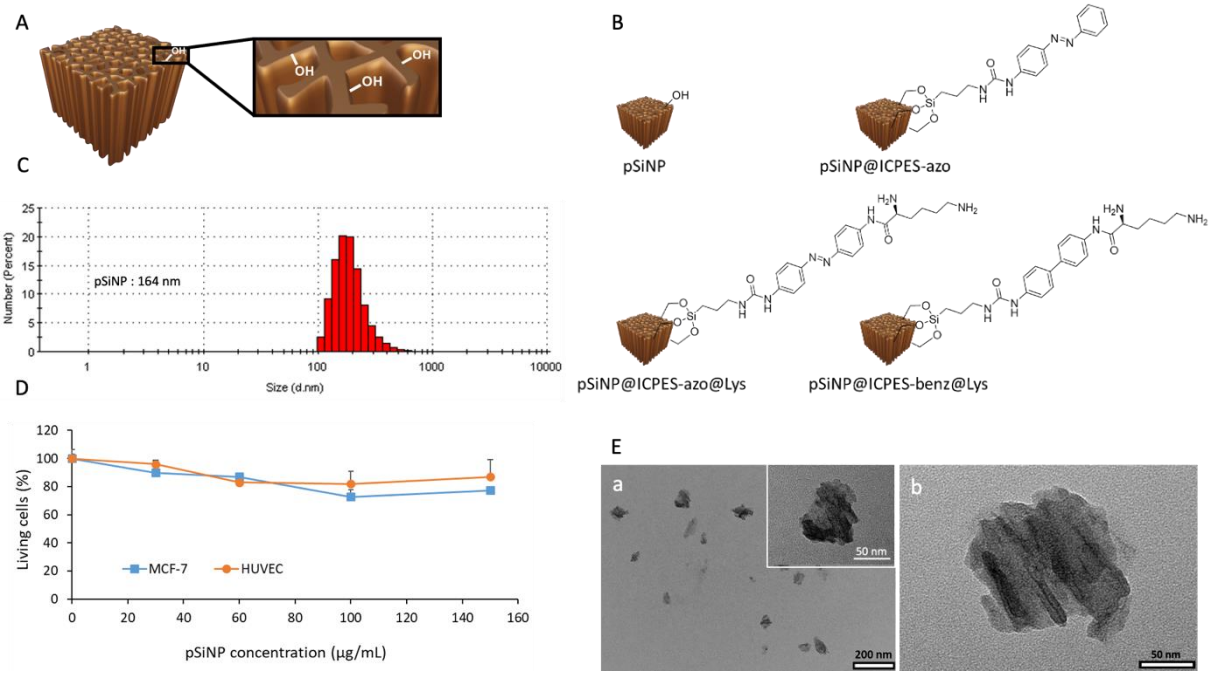

Figure 1. (A) Schematic representation of pSiNP. (B) Schematic representation of the 4 formulations: pSiNP, pSiNP@ICPES-azo, pSiNP@ICPES-azo@Lys, pSiNP@ICPES-benz@Lys. Off-scale representation. The organic ligands are grafted at both the internal and external surfaces of the pSiNP. (C) Particle size distribution in number measured by dynamic light scattering (DLS) for pSiNP (164 nm). (D) Cytotoxicity study of pSiNP on MCF-7 and on HUVEC cells. Cells seeded in 96 well-plate were incubated 72 h with increasing concentrations of pSiNP (from 30 to 150 µg.ml^{-1}). Cell viability was established by MTT test. Values are means ± standard deviations. (E) TEM images of pSiNP. (a) At different magnifications. Scale bars are 200 nm and 50 nm (insert) (b) Same sample, different field. Scale bar is 50 nm.

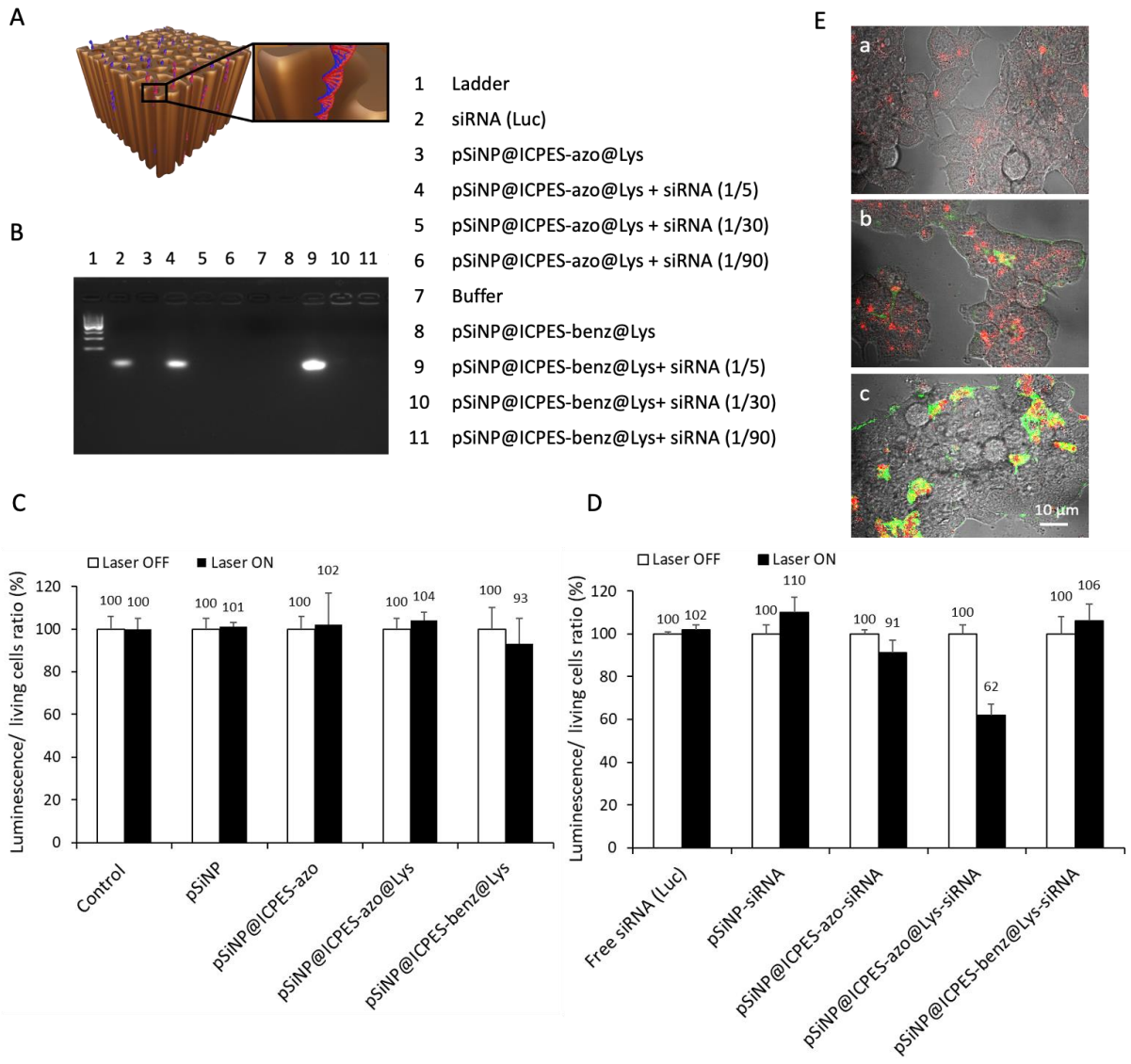

Figure 2. (A) Schematic representation of siRNA complexation in chemically functionalized pSiNP. (B) Gel retardation assay image for the nanoformulations. Exposure time was 120 ms.

(C-D) Transfection efficiency of the nanoformulations upon TPE-triggered siRNA delivery in MCF-7 Luc breast cancer cells: (C) negative control without siRNA, (D) Luciferase silencing test for free siRNA, pSiNP + siRNA, pSiNP@ICPES-azo + siRNA, pSiNP@ICPES-azo@Lys + siRNA, and pSiNP@ICPES-benz@Lys + siRNA. 1/25 weight ratio was selected for each nanoformulation. Data are mean values ±

standard deviations from three independent experiments. (E) Confocal microscopy imaging of (a) MCF-7 cells stained with lysotracker, (b) MCF-7 cells stained with lysotracker and incubated with free siRNA-ATTO (160 nM), and (c) MCF-7 cells stained with lysotracker and incubated with siRNA-ATTO complexed with pSiNP@ICPES-azo@Lys (weight ratio 1/25, siRNA/nanoparticle).

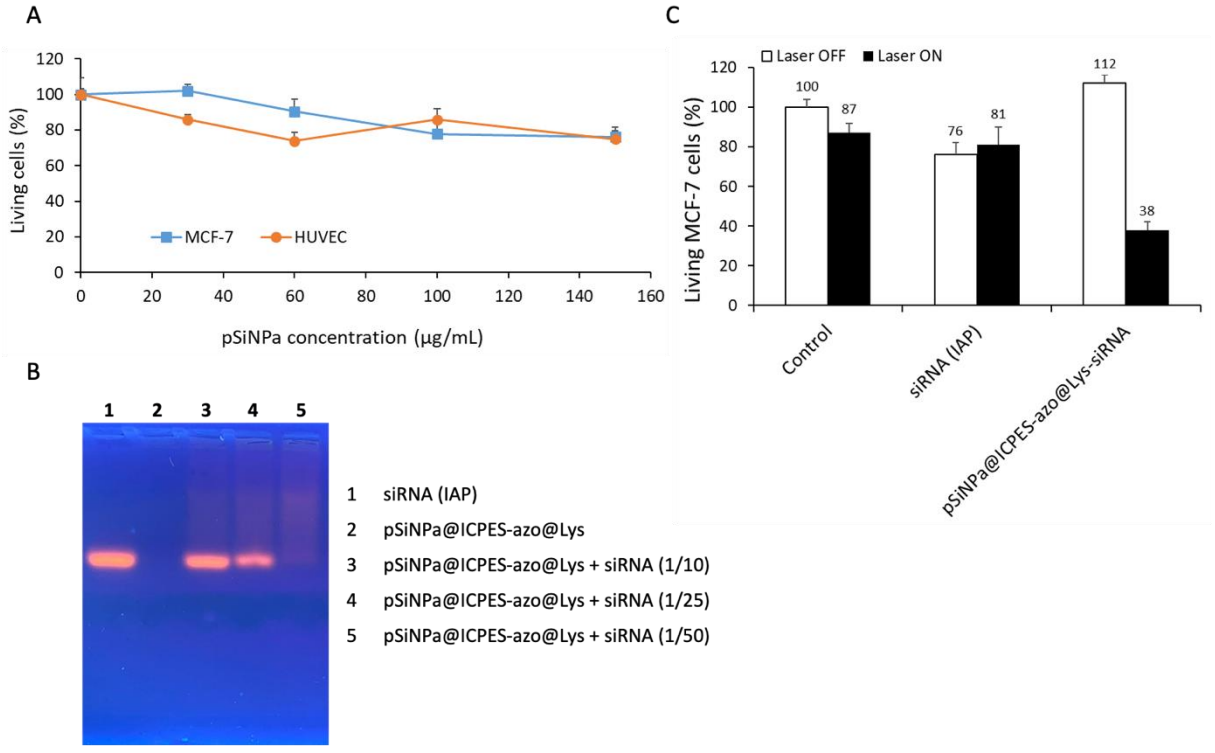

Figure 3. (A) Cytotoxicity study of pSiNPa on MCF-7 and on HUVEC cells. Cells seeded in 96 well-plate were incubated 72 h with increasing concentrations of pSiNPa (from 30 to 150 µg.ml^{-1}). Cell viability was established by MTT test. Values are means ± standard deviations. (B) Gel retardation assay image for the nanoformulations. (C) Transfection efficiency of siRNA (IAP) upon TPE-triggered delivery in MCF-7 breast cancer cells.

3. Conclusion

Biocompatible porous silicon nanoparticles, chemically functionalized with positively charged lysine-azobenzene groups, can efficiently complex and deliver siRNA to MCF-7 breast cancer cell upon two-photon excitation light. Release of siRNA in the cancer cells and gene silencing is triggered by the photo-isomerization of the lysine-functionalized azobenzene only when irradiated, with resonance energy transfer from pSiNP. The pSiNP@ICPES-azo@Lys functionalized nanovector of the present study (1) is biocompatible, biodegradable and non-toxic to the cells, (2) allows safe cellular internalization of siRNA, (3) maintains it inactive in the cells until it is irradiated, (4) delivers it in the cytoplasm of the cells with a short irradiation time (seconds), upon absorption of non-harmful TPE-NIR light, and (5) allows high-efficiency siRNA transfection (>70%). It constitutes a potent light triggered system and safe non-viral vector to spatiotemporally control gene transfection. It brings an interesting insight in cancer therapy with potential important advances in precision nanomedicine, in combination with recently described two-photon endoscopes. [20]

4. Experimental Methods

4.1. Preparation and characterization of the nanoformulations

4.1.1. Coupling reaction between Boc-lysine(Boc)-OH and 4,4'-diaminoazobenzene

Hydroxybenzotriazole (115 mg, 0,851 mmol) and *N*,*N*'-dicyclohexylcarbodiimide (175 mg, 0,848 mmol) were mixed in a solution of Boc-Lys(Boc)-OH (264 mg, 0,5 mmol) in anhydrous DMF (5 ml) at room temperature under nitrogen flux. After 1 h, 4,4'-diaminoazobenzene (150 mg, 0,707 mmol) was

added to the reaction and mixed at room temperature overnight. The mixture was then diluted in a sodium chloride solution and extracted with ethyl acetate (EtOAc). The obtained product was dried on $MgSO_4$ and the solvent eliminated under vacuum. The residue was purified by column chromatography (eluant: DCM : EtOAc (70 % : 30 %)). **Yield**: 35 %. **^{1}H NMR** (400 MHz, CDCl3) : 1.26 (m, 2H), 1.46 (d, 18H), 1.55 (m, 2H), 1.95 (m, 2H), 3.15 (q, 2 H), 4.02 (br,1H), 4.20 (br, 1H), 4.63 (m, 1H), 5.21 (br, 1H), 6.74 (d, 2H), 7.67 (d, 2H), 7.78 (d, 2H), 7.83(d, 2H), 8.63 (br, 1H). **MS (MALDI)**: calculated for $C_{28}H_{35}N_7O_5$ [M + H] + m/z 541,31; obtained m/z 541,31 and **HRMS** obtained m/z 541,3140 (ESI Figure **S1** and **S2**).

4.1.2. Coupling reaction between azo@Lys(diBoc) and 3-isocyanopropyltriethoxysilane, and grafting to the pSiNP

3-isocyanopropyltriethoxysilane (ICPES) (4,6 µL, 0,018 mmol) was added to a solution of azo@Lys(diBoc) (10 mg, 0,018 mmol) in anhydrous THF (3 ml). The reaction was mixed for 24 h under nitrogen flux. After removal of the solvent, the obtained product ICPES-azo@Lys(diBoc) was added to a suspension of 25 mg of pSiNP in 3,5 ml of toluene. The reaction was mixed at 50°C for 24h under nitrogen flux. The nanoparticles were centrifuged for 15 min at 14000 rpm then collected and rinsed three times in absolute ethanol. For the deprotection of lysine, the nanoparticles were resuspended in 2 ml of a TFA: CH_2Cl_2 (40% : 60%) solution for 30 min. Coupling reaction yield was determined by UV-Visible spectroscopy. The reaction scheme for the prepared as called formulation pSiNP@ICPES-azo@Lys is presented in ESI Figure **S3**.

4.1.3 Coupling reaction between 4-aminoazobenzene and 3-isocyanopropyltriethoxysilane and grafting to the pSiNP

20 mg of 4-aminoazobenzene and 25 µL of ICPES were added to 3 ml of anhydrous THF. The reaction was mixed for 24 h under nitrogen flux. The obtained product, ICPES-azo was dried and then added to a suspension of 25 mg of pSiNP in 3.5 ml of toluene. The reaction was mixed at 50°C for 24h under nitrogen flux. Coupling reaction yield was determined by UV-Visible spectroscopy. The reaction scheme for the prepared as called formulation pSiNP@ICPES-azo is presented in ESI Figure **S4**.

4.1.4. Coupling reaction between Boc-lysine(Boc)-OH and 1,4-4' diaminodiphenyl

Benzidine (120 mg, 0.65 mmol) was dissolved in 4 ml of DMF anhydrous. After that, N^2, N^6-bis(tert-butoxycarbonyl)-D-lysine (380 mg, 0.72 mmol), (Benzotriazol-1-yloxy)tripyrrolidinophosphonium hexafluorophosphate (375 mg, 0.75 mmol) and *N*,*N* diisopropylethylamine (125 μl, 0.72 mmol) were successively added. The reaction was then kept under stirring at room temperature for 18 h. Thereafter, the solvent was evaporated, and the crude solid was washed with brine (50 ml) and extracted with DCM (2 x 50 ml). The collected organic phase was dried over $MgSO_4$, filtered and concentrated under vacuum. The viscous solid crude was purified by flash chromatography column (SiO_2; gradient from 0–50% AcOEt in CH_2Cl_2) to afford di-tert-butyl(6-((4'-amino-[1,1'-biphenyl]-4-yl)amino)-6-oxohexane-1,5-diyl)(R)-dicarbamate as called (benz@Lys(diBoc) as a white powder (280 mg, 84%) (ESI Figure **S5**). **^{1}H NMR** (500.1 MHz, DMSO-d^6): δ 9.92 (s, 1H), 7.67 (d, *J*=8,8 Hz, 1H), 7.60-7.57 (m, 3H), 7.46 (d, *J*=8,7 Hz, 2H), 7.31 (d, *J*=8.6 Hz, 2H), 6.97-6.93 (m, 1H), 6.75 (t, *J*=5.2 Hz, 1H), 6.62 (d, *J*=6.6 Hz, 2H), 5.15 (s, 2H), 4.04 (t, *J*=4.9 Hz, 1H), 2.92-2.84 (m, 2H), 2.00-1.94 (m, 2H), 1.38 (s, 9H), 1.36 (s, 9H), 1.11-1.07 (m, 2H) . **^{13}C NMR** (125.7 MHz, DMSO-d^6): δ 171.7, 155.9, 155.8, 147.9, 138.1, 136.9, 135.6, 134.4, 127,1, 126.7, 126.4, 125.4, 119.5, 114.2, 78.0, 77.3, 55.1, 52.1, 31.6, 29.2, 28.3, 28.2, 23.9. **HMRS**: *m*/*z*: calcd for $C_{28}H_{40}N_4O_5$ $[M]^+$: 512,3021; found: 513,3187 $[M+H]^+$ (ESI Figure **S6**).

4.1.5. Coupling reaction between benz@Lys(diBoc) and 3-isocyanopropyltriethoxysilane, and grafting to the pSiNP.

Triethoxy(3-isocyanatopropyl)silane (55 μL, 0.22 mmol) was added to a solution of di-tert-butyl(6-((4'-amino-[1,1'-biphenyl]-4-yl)amino)-6-oxohexane-1,5-diyl)(R)-dicarbamate (103 mg, 0.2 mmol) in THF anhydrous and was kept under stirring at 70ºC for 24 h. After that, the solvent was removed under reduced pressure and the crude solid was gently washed with a pentane/diethyl ether mixture. di-tert-butyl(6-oxo-6-((4'-(3-(3-(triethoxysilyl)propyl)ureido)-[1,1'-biphenyl]-4-yl)amino)hexane-1,5-diyl)(R)-dicarbamate as called (ICPES-benz@Lys(diBoc) was afforded as a pale orange powder (123 mg, 81 %) (ESI Figure **S7**). **^{1}H NMR** (500.1 MHz, DMSO-d^6): δ 9.97 (s, 1H), 8.46 (s, 1H), 7.65-7.43 (m, 8H), 6.98 (s, 1H), 6.77 (s, 1H), 6.17 (s, 1H), 4.05 (bs, 1H), 3.77-3.71 (m, 6H), 3.08-

3.04 (m, 2H), 2.91-2.88 (m, 2H), 1.77-1.74 (m, 2H), 1.64-1.57 (m, 2H), 1.52-1.46 (m, 2H), 1.39 (s, 9H), 1.36 (s, 9H), 1.16-1.13 (m, 8H), 0.58-0.55 (m, 2H). **^{13}C NMR** (125.7 MHz, DMSO-d^6): δ 171.4, 155.1, 139.8, 137.8, 134.8 132.2, 126.4, 126.1, 119.5, 117.9, 78.0, 77.3, 57.7, 55.1, 41.7, 31.5, 29.2, 28.3, 28.2, 23.3, 22.9, 18.2, 7.3. **^{29}Si NMR** (99.3 MHz, DMSO-d^6): δ -45.2. **MALDI-TOF**: *m/z*: calcd for $C_{38}H_{61}N_5O_9Si$ $[M]^+$: 759,413; found: 782,402 $[M+Na]^+$ (ESI Figure **S8**).

The obtained product was dried and then added to a suspension of 25 mg of pSiNP in 3.5 ml of toluene. The reaction was mixed at 50°C for 24h under nitrogen flux. The nanoparticles were centrifuged for 15 min at 14000 rpm then collected and rinsed three times in absolute ethanol. For the deprotection of lysine, the nanoparticles were resuspended in 2 ml of a TFA: CH_2Cl_2 (40% : 60%) solution for 30 min. Coupling reaction yield was determined by UV-Visible spectroscopy. The reaction scheme for the prepared as called formulation pSiNP@ICPES-benz@Lys is presented in ESI Figure **S7**.

4.1.6. Synthesis of the pSiNP for transfection experiments

Boron-doped p^{++}-type Si (0.8-1.2 mΩ.cm resistivity, <100> orientation) from Siltronix (France) was electrochemically etched in a 3:1 (v:v) solution of aqueous 48% hydrofluoric acid (HF):absolute ethanol (Sigma-Aldrich). Etching was performed in a Teflon cell with a platinum ring counter electrode. A constant current of 200 mA.cm^{-2} was applied for 150 s, and then the sample was rinsed 3 times with ethanol. The porous layer was then removed from the substrate by application of an electropolishing current of 4 mA.cm^{-2} for 250 s in an electrolyte solution containing 1:20 (v:v) aqueous 48% hydrofluoric acid:absolute ethanol. After 3 rinses with ethanol, the porous layer was placed in ethanol in a glass vial. After degassing the sample for 20 min under a nitrogen stream, the porous silicon film was fractured by ultrasonication during 16 h. The largest particles were then removed by spinning them down by centrifugation at 3,000 rpm for 2 min (Minizine, Eppendorf). In order to remove the smallest particles, the solution was finally centrifuged at 14000 rpm for 30 min (centrifuge Eppendorf 5804). The pellet was then re-dispersed in absolute ethanol.

4.1.7. Synthesis of the pSiNP for cancer therapy

Porous silicon films were anodized from 100 mm boron-doped p+ type Si (100)-oriented wafers (University Wafers Inc, USA) with a resistivity of 0.01 - 0.02 Ω cm in an electrolyte solution of

hydrofluoric acid (HF, 50%, VLSI Selectipur®, 7664-39-3) and absolute ethanol (99%, Sigma-Aldrich, 32221) in a 1:2 volumetric ratio. Electrochemical etching of porous multilayers was carried out in a custom-made Teflon etch cell with the backside of the wafer in contact with an aluminium sheet and the front side of the wafer exposed to the anodizing electrolyte. A platinum mesh was used as the counter electrode over the polished silicon wafer surface. Each etching cycle consisted of two current densities applied successively: 42 mA/cm^2 for 3 s, followed by 168 mA/cm^2 for 0.35 s. The cycle was repeated 360 times, and then, a lift-off layer was generated using 246 mA/cm^2 for 1 s. The pSi films were then scrapped from the wafer and fractured by probe sonication (Sonics & Materials™ Ultrasonic Processor model VCX130) in isopropanol (IPA, Sigma-Aldrich, 59300) for 6 hours, 70% power with 4 s ON and 4 s OFF. The resulting dispersion of pSi nanoparticles was centrifuged for 5 minutes at 20000 rcf and the pellet was redispersed in IPA via sonication for a few seconds. The resulting dispersion was centrifuged at 1300 rcf for 5 minutes and the supernatant solution containing the particles of the desired size was collected. This step was repeated 5 times until the supernatant was almost clear. PSiNP of 190 nm in size with a polydispersity of 0.22 and a surface charge of -20 mV were obtained.

4.1.8. Characterization of the pSiNP by transmission electron microscopy

Transmission Electron Microscope (TEM) images were obtained using a Jeol 1200 EX II microscope.

4.1.9. Characterization of the pSiNP by nitrogen sorption analysis

Nitrogen adsorption-desorption isotherms of the pSi nanoparticles were recorded at 77K using a micromeritics ASAP 2020 volumetric apparatus. Prior to the adsorption experiment, the samples were outgassed overnight *in situ* at 303 K (ESI Figure **S10**).

4.1.10. Characterization of the pSiNP by dynamic light scattering

The DLS measurements were performed in ethanol and in DMEM + 10% FCS at a concentration of 1 mg.ml^{-1} and of 150 µg.ml^{-1} (the concentration used for the biological experiments), on a Malvern nanozetasizer instrument (ESI Figure **S11**).

4.1.11. Characterization of the nanoformulations by Fourier transform infrared spectroscopy

Infrared spectra were recorded on Nicolet IS5 spectrometer with the ATR ID5 module (ESI Figure **S12, S13** and **S14**).

4.1.12. Characterization of the nanoformulations by zeta potential measurements

Two drops of diluted functionalized porous silicon nanoparticles in deionised water were added to 1 mL of deionised water. The zeta potential measurements of the functionalized pSiNP were performed on a Malvern Nanozetasizer instrument (ESI Table **S1**).

4.1.13. Quantification of the grafted moieties at the surface of the pSiNP

Quantification of the ICPES-azo, ICPES-azo@Lys and ICPES-benz@Lys molecules grafted on the pSiNP was determined spectrophotometrically after dissolution of a known amount of nanoparticle formulations in an aqueous basic solution of KOH 1M. The UV-Vis absorption measurements were performed with a Lambda 35 de Perkin Elmer spectrometer. The absorbance was monitored at 379 nm in the case of the azobenzene derivatives, whereas it was detected at 295 nm for the benzidine-based compound ICPES-benz@Lys. Absorbance of standard solutions of azobenzene at determined concentrations in KOH 1M was measured, allowing to plot a calibration curve. Molar extinction coefficient for azobenzene and benzidine was determined at $\varepsilon = 1{,}7 \times 10^4$ $mol^{-1}.cm^{-1}$, and $\varepsilon = 2{,}4 \times 10^4$ $mol^{-1}.cm^{-1}$ respectively (ESI Table **S2**).

4.1.14. Gel retardation assay

Various ratios of pSiNP@ICPES-azo@Lys or pSiNP@ICPES-benz@Lys and siRNA were mixed in a total volume of 22.5 µl and incubated 30 min at room temperature to induce the complexation with siRNA. Then, 10 µl of the samples were added with xylene blue (4 µL) and deposited on agarose gel (2.5%). Samples were submitted to migration (30 min; 50 V). Delayed migration of siRNA demonstrated the complexation with pSiNP. The staining was performed by GelRed under the experimental conditions described by the manufacturer (FluoProbes®).

4.2. Photocontrolled siRNA delivery upon TPE and transfection efficiency

4.2.1. Cell culture and cytotoxicity study

For cell culture, Human breast adenocarcinoma cells (MCF-7) were purchased from ATCC and cultured in Dulbecco's Modified Eagle's Medium (DMEM) supplemented with 10% fetal bovine serum (FBS) and 1% penicillin/streptomycin (P/S). For MCF-7/firefly luciferase (MCF-7 Luc) stable cells express transgenically firefly luciferase. They were cultivated in F12-DMEM supplemented with 10% fetal bovine serum (FBS) and 2% geneticin (for gene selection). Cell types were then grown in humidified atmosphere at 37 °C under 5% CO_2. Human Umbilical Vein Endothelial Cells (HUVEC) were cultivated in the same conditions of temperature and CO2. The culture medium is Endothelial Cell Growth Medium (211-500) supplemented with 10% fetal bovine serum (FBS) and 1% P/S.

For cytotoxicity experiment, cells were seeded in 96-well plates at a density of 2000 cells per well. Twenty-four hours after cell growth, cells were treated with different concentrations of pSiNP (from 0 to 150 $\mu g.ml^{-1}$). After 3 days of incubation, cell viability was assessed by a MTT assay. Briefly cells were incubated in the presence of 0.5 $mg.ml^{-1}$ MTT during 3 h to determine mitochondrial enzyme activity. Then, MTT precipitates were dissolved in 150 µL of an ethanol/DMSO (1:1) solution and absorbance was read at 540 nm.

4.2.2. Confocal microcopy imaging

MCF-7 cells were stained with lysotracker red DND-99 (Thermofisher ref L7528) in accordance with the manufacturer protocol and incubated with free siRNA (160 nM) or siRNA complexed with pSiNP@ICPES-azo@Lys (ratio 1/25) for 24 hours. Cells were imaged with LSM 780 confocal microscope. Pictures are merged images of transmission and fluorescence imaging. Lysotracker (red) was excited at 561 nm and siRNA ATTO (green) at 488 nm.

4.2.3. TPE-triggered siRNA delivery

The siRNA solution was prepared with RNase-free water at a concentration of 20 µM. pSiNP samples were diluted in ethanol to a concentration of 1 $mg.ml^{-1}$. Then, the complexation was carried out in milliQ water in the indicated ratio, for 30 min at room temperature. Finally, the complexes were added at 40 $\mu g.ml^{-1}$ (concentration of pSiNP) in the culture medium of the cancer cells. The different types of pSiNP, complexed or not with siRNAs at 1/25 (siRNA (Luc)) or 1/50 (siRNA (IAP)) weight ratio, were incubated during 5 h at 40 $\mu g.ml^{-1}$ with seeded cells in 384 multiwell glass-bottom plate.

Then, cells were submitted or not to laser irradiation with a confocal Carl Zeiss two-photon microscope at 800 nm and maximum laser power (3W input, 1100 mW output at lens). Half of the wells was irradiated at 800 nm by three scans of 1.57 s duration in four different areas of the well. The laser beam was focused by a microscope objective lens (Carl Zeiss 10-fold magnification /objective 0.3 EC Plan-Neofluar). For siRNA (Luc), after 2 days, luciferase activity was assessed by addition into the culture medium of luciferin (10^{-3} M, final concentration) purchased from Promega (France). Living cell luminescence was measured 10 min after by a CLARIOstar multilabel plate reader. Results were corrected according to the following formula Lum non-irradiated - 2 (Lum non irradiated – Lum irradiated), where Lum is the luminescence emitted. Values are expressed as a percentage of luciferase activity compared to non-irradiated well (set as 100%) corrected by viability assessed by MTT assay (performed as previously described). For siRNA (IAP), two days after TPE, cell death was quantified by MTT test.

4.2.4. Quenching of pSiNP with azobenzene

Steady-state photoluminescence spectra were obtained using an Ocean Optics QE65 Pro spectrophotometer fitted with a 500 nm long-pass filter on the inlet. The excitation source was a UV LED operating at 375 nm with a nominal output power of 5 mW. The pSiNP were immersed in 1 ml of EtOH solution in a glass vial. Aliquots of an ethanolic solution of azobenzene at different concentrations (0.5 mM to 1.95 mM) were added to the pSiNP suspension using a microliter syringe, and the mixture was stirred for 1 min (ESI Figure **S15**).

Supporting Information

Supporting Information is available from the Wiley Online Library or from the author.

Acknowledgements

FC gratefully acknowledges the University of Montpellier and the French Ministry PhD programme (2018-2021), the Carnot Institut (CED2) and LabEx CheMISyst programme (2012-2015) for financial support. The NETPORE COST programme is acknowledged for the STSM grant to CS. CC acknowledges support from the ERC Starting Grant ENBION 759577.

We acknowledge the imaging facility MRI, member of the national infrastructure France-BioImaging infrastructure supported by the French National Research Agency (ANR-10-INBS-04 «Investments for the future».

Author 1, author 2 and Author 3 contributed equally to this work.

Received: ((will be filled in by the editorial staff))
Revised: ((will be filled in by the editorial staff))
Published online: ((will be filled in by the editorial staff))

References

[1] S. Huang, M. Kamihira, *Biotechnol. Adv.* **2013**, *31*, 208-223.

[2] a) G. Lin, L. Li, N. Panwar, J. Wang, S. C. Tjin, X. Wang, K.-T. Yong, *Coord. Chem. Rev.* **2018**, *374*, 133-152; b) M. Foldvari, D. W. Chen, N. Nafissi, D. Calderon, L. Narsineni, A. Rafiee, *J. Control. Release.* **2016**, *240*, 165-190.

[3] a) A. Garcia-Guerra, T. L. Dunwell, S. Trigueros, *Curr Med Chem* **2018**, *25*, 2448-2464; b) H.-K. Na, M.-H. Kim, K. Park, S.-R. Ryoo, K. E. Lee, H. Jeon, R. Ryoo, C. Hyeon, D.-H. Min, *Small* **2012**, *8*, 1752-1761.

[4] a) L. Cheng, E. Anglin, F. Cunin, D. Kim, M. J. Sailor, I. Falkenstein, A. Tammewar, W. R. Freeman, *Br. J. Ophthalmol.* **2008**, *92*, 705-711; b) S. P. Low, K. A. Williams, L. T. Canham, N. H. Voelcker, *Biomaterials* **2006**, *27*, 4538-4546; c) S. H. C. Anderson, H. Elliott, D. J. Wallis, L. T. Canham, J. J. Powell, *physica status solidi (a)* **2003**, *197*, 331-335; d) J. F. Popplewell, S. J.

King, J. P. Day, P. Ackrill, L. K. Fifield, R. G. Cresswell, M. L. di Tada, K. Liu, *Journal of Inorganic Biochemistry* **1998**, *69*, 177-180.

[5] E. Secret, M. Maynadier, A. Gallud, A. Chaix, E. Bouffard, M. Gary-Bobo, N. Marcotte, O. Mongin, K. El Cheikh, V. Hugues, M. Auffan, C. Frochot, A. Morere, P. Maillard, M. Blanchard-Desce, M. J. Sailor, M. Garcia, J.-O. Durand, F. Cunin, *Adv. Mater.* **2014**, *26*, 7643-7648.

[6] C. Spiteri, V. Caprettini, C. Chiappini, *Biomater. Sci.* **2020**, *8*, 6992-7013.

[7] a) A. Estevez-Torres, C. Crozatier, A. Diguet, T. Hara, H. Saito, K. Yoshikawa, D. Baigl, *Proc. Natl. Acad. Sci. U S A* **2009**, *106*, 12219-12223; b) S. Rudiuk, H. Saito, T. Hara, T. Inoue, K. Yoshikawa, D. Baigl, *Biomacromolecules* **2011**, *12*, 3945-3951.

[8] a) H. D. Do, B. M. Couillaud, B. T. Doan, Y. Corvis, N. Mignet, *Adv Drug Deliv Rev* **2019**, *138*, 3-17; b) L. M. A. Ali, M. Gary-Bobo, *Cancers* **2022**, *14*, 3597.

[9] a) N. Laroui, M. Coste, L. Lichon, Y. Bessin, M. Gary-Bobo, G. Pratviel, C. Bonduelle, N. Bettache, S. Ulrich, *Int. J. Pharm. (Amsterdam, Neth.)* **2019**, *569*, 118585; b) L. Yu, D. Liang, C. Chen, X. Tang, *Biomacromolecules* **2018**, *19*, 2526-2534; c) J. Wang, L. Xie, T. Wang, F. Wu, J. Meng, J. Liu, H. Xu, *Acta Biomater.* **2017**, *59*, 158-169; d) S. P. Patil, B. A. Moosa, S. Alsaiari, K. Alamoudi, A. Alshamsan, A. Al Malik, K. Adil, M. Eddaoudi, N. M. Khashab, *Chem. - Eur. J.* **2016**, *22*, 13789-13793; e) A. A. Foster, C. T. Greco, M. D. Green, T. H. Epps, III, M. O. Sullivan, *Adv. Healthc. Mater.* **2015**, *4*, 760-770; f) F. Buhr, J. Kohl-Landgraf, S. T. Dieck, C. Hanus, D. Chatterjee, A. Hegelein, E. M. Schuman, J. Wachtveitl, H. Schwalbe, *Angew. Chem. Int. Ed. Engl.* **2015**, *54*, 3717-3721; g) J. Zheng, Y. Nie, S. Yang, Y. Xiao, J. Li, Y. Li, R. Yang, *Analytical Chemistry* **2014**, *86*, 10208-10214; h) H.-J. Li, H.-X. Wang, C.-Y. Sun, J.-Z. Du, J. Wang, *Rsc Advances* **2014**, *4*, 1961-1964; i) M. D. Green, A. A. Foster, C. T. Greco, R. Roy, R. M. Lehr, T. H. Epps, III, M. O. Sullivan, *Polymer Chemistry* **2014**, *5*, 5535-5541; j) L. Yin, H. Tang, K. H. Kim, N. Zheng, Z. Song, N. P. Gabrielson, H. Lu, J. Cheng, *Angew. Chem. Int. Ed. Engl.* **2013**, *52*, 9182-9186.

[10] a) J. Li, C. W. T. Leung, D. S. H. Wong, J. Xu, R. Li, Y. Zhao, C. Y. Y. Yung, E. Zhao, B. Z. Tang, L. Bian, *ACS Appl. Mater. Interfaces* **2019**, *11*, 22074-22084; b) M. K. G. Jayakumar, A. Bansal, K. Huang, R. Yao, B. N. Li, Y. Zhang, *Acs Nano* **2014**, *8*, 4848-4858; c) Y. Yang, F. Liu, X. Liu, B. Xing, *Nanoscale* **2013**, *5*, 231-238; d) M. K. G. Jayakumar, N. M. Idris, Y. Zhang, *Proc. Natl. Acad. Sci. U S A* **2012**, *109*, 8483-8488.

[11] G. Chen, B. Ma, R. Xie, Y. Wang, K. Dou, S. Gong, *J. Control. Release.* **2018**, *282*, 148-155.

[12] a) A. Gnach, T. Lipinski, A. Bednarkiewicz, J. Rybka, J. A. Capobianco, *Chemical Society Reviews* **2015**, *44*, 1561-1584; b) I. Blinova, M. Muna, M. Heinlaan, A. Lukjanova, A. Kahru, *Nanomaterials* **2020**, *10*, 328.

[13] a) E. Morgan, D. Wupperfeld, D. Morales, N. Reich, *Bioconjug. Chem.* **2019**, *30*, 853-860; b) R. S. Riley, M. N. Dang, M. M. Billingsley, B. Abraham, L. Gundlach, E. S. Day, *Nano Lett.* **2018**, *18*, 3565-3570; c) F. Yin, C. Yang, Q. Wang, S. Zeng, R. Hu, G. Lin, J. Tian, S. Hu, R. F. Lan, H. S. Yoon, F. Lu, K. Wang, K.-T. Yong, *Theranostics* **2015**, *5*, 818-833; d) X. Huang, Q. Hu, G. B. Braun, A. Pallaoro, D. P. Morales, J. Zasadzinski, D. O. Clegg, N. O. Reich, *Biomaterials* **2015**, *63*, 70-79; e) X. Huang, A. Pallaoro, G. B. Braun, D. P. Morales, M. O. Ogunyankin, J. Zagadzinski, N. O. Reich, *Nano Lett.* **2014**, *14*, 2046-2051; f) R. Huschka, A. Barhoumi, Q. Liu, J. A. Roth, L. Ji, N. J. Halas, *Acs Nano* **2012**, *6*, 7681-7691; g) Y.-T. Chang, P.-Y. Liao, H.-S. Sheu, Y.-J. Tseng, F.-Y. Cheng, C.-S. Yeh, *Advanced Materials* **2012**, *24*, 3309-3314.

[14] Y. Yang, Y. Yang, X. Xie, Z. Wang, W. Gong, H. Zhang, Y. Li, F. Yu, Z. Li, X. Mei, *Biomaterials* **2015**, *48*, 84-96.

[15] E. J. Cueto Diaz, S. Picard, V. Chevasson, J. Daniel, V. Hugues, O. Mongin, E. Genin, M. Blanchard-Desce, *Org. Lett.* **2015**, *17*, 102-105.

[16] H. Zhao, H. Tao, W. Hu, X. Miao, Y. Tang, T. He, J. Li, Q. Wang, L. Guo, X. Lu, W. Huang, Q. Fan, *ACS Applied Bio Materials* **2019**, *2*, 1676-1685.

[17] a) J. Croissant, M. Maynadier, A. Gallud, H. P. N'Dongo, J. L. Nyalosaso, G. Derrien, C. Charnay, J.-O. Durand, L. Raehm, F. Serein-Spirau, N. Cheminet, T. Jarrosson, O. Mongin, M. Blanchard-Desce, M. Gary-Bobo, M. Garcia, J. Lu, F. Tamanoi, D. Tarn, T. M. Guardado-Alvarez, J. I. Zink, *Angew. Chem. Int. Ed.* **2013**, *52*, 13813-13817; b) L. De Boni, J. J. Rodrigues, D. S. dos Santos, C. H. T. P. Silva, D. T. Balogh, O. N. Oliveira, S. C. Zilio, L. Misoguti, C. R. Mendonça, *Chem. Phys. Lett.* **2002**, *361*, 209-213.

[18] M. K. A. Rahim, T. Fukaminato, T. Kamei, N. Tamaoki, *Langmuir* **2011**, *27*, 10347-10350.

[19] S. Angelos, E. Choi, F. Voegtle, L. De Cola, J. I. Zink, *J. Phys. Chem. C* **2007**, *111*, 6589-6592.

[20] R. Won, *Nat. Photonics* **2016**, *10*, 73.

[21] J. Lu, E. Choi, F. Tamanoi, J. I. Zink, *Small* **2008**, *4*, 421-426.

A potent two-photon light triggered system made of chemically functionalized porous silicon nanoparticles is designed as a safe non-viral vector for the spatiotemporal control of gene transfection in cancer therapy.

A. Chaix, E. Cueto-Diaz, S. Dominguez-Gil, C. Spiteri, L. Lichon, M. Maynadier, X. Dumail, D. Aggad, A. Delalande, A. Bessière, C. Pichon, C. Chiappini, M. J. Sailor, N. Bettache, M. Gary-Bobo, J.-O. Durand, C. Nguyen,* F. Cunin*

Two-photon light trigger siRNA transfection of cancer cells using non-toxic porous silicon nanoparticles